TISSUE ENGINEERING: Part A
Volume 19, Numbers 3 and 4, 2013

DOI: 10.1089/ten.tea.2012.0072

Scaffold Fiber Diameter Regulates Human Tendon Fibroblast Growth and Differentiation

Cevat Erisken, PhD,[1] Xin Zhang, MS,[1] Kristen L. Moffat, PhD,[1]
William N. Levine, MD,[2] and Helen H. Lu, PhD[1]

The diameter of collagen fibrils in connective tissues, such as tendons and ligaments is known to decrease upon injury or with age, leading to inferior biomechanical properties and poor healing capacity. This study tests the hypotheses that scaffold fiber diameter modulates the response of human tendon fibroblasts, and that diameter-dependent cell responses are analogous to those seen in healthy versus healing tissues. Particularly, the effect of the fiber diameter (320 nm, 680 nm, and 1.80 μm) on scaffold properties and the response of human tendon fibroblasts were determined over 4 weeks of culture. It was observed that scaffold mechanical properties, cell proliferation, matrix production, and differentiation were regulated by changes in the fiber diameter. More specifically, a higher cell number, total collagen, and proteoglycan production were found on the nanofiber scaffolds, while microfibers promoted the expression of phenotypic markers of tendon fibroblasts, such as collagen I, III, V, and tenomodulin. It is possible that the nanofiber scaffolds of this study resemble the matrix in a state of injury, stimulating the cells for matrix deposition as part of the repair process, while microfibers represent the healthy matrix with micron-sized collagen bundles, thereby inducing cells to maintain the fibroblastic phenotype. The results of this study demonstrate that controlling the scaffold fiber diameter is critical in the design of scaffolds for functional and guided connective tissue repair, and provide new insights into the role of matrix parameters in guiding soft tissue healing.

Introduction

Connective tissues, such as tendons and ligaments that join muscle to bone and bone to bone, respectively, are ubiquitous in the body and play critical roles in musculoskeletal mechanics. In these soft tissues, the smallest structural unit is the collagen molecule with a size of about 1 nm,[1] which assembles into fibrils with diameters up to 360 nm,[2] which then come together to form collagen fibers (1–300 μm).[3] These fibers are subsequently bundled to form fascicles (150–1000 μm),[4] which populate the collagenous matrix. Injuries associated with these connective tissues are common, with over 250,000 rotator cuff tendon repairs and more than 100,000 anterior cruciate ligament reconstructions performed annually in the United States.[5,6] Soft tissue healing often results in the formation of a scar tissue, which is compositionally and mechanically inferior to the native tendon or ligament,[7] resulting in as high as 94% recurrent tears in some cases.[8]

The diameter of collagen fibers has been reported to vary with the health (Table 1)[2,3,9–12] and age.[13] Formation of the scar tissue is generally accompanied by a decrease in the average diameter of collagen fibrils,[14] which makes up the backbone of the extracellular matrix of tendons or ligaments.[15] For example, characterization of the injured and healthy tendon in terms of collagen fibril/fiber diameter and organization revealed an extracellular matrix consisting largely of smaller diameter collagen fibrils or disorganized structures once the tissue has been injured.[2,9] The reduction in the fibril diameter is believed to be associated with overloading at the time of injury, which causes chemical modification of the covalent crosslinks between collagen molecules so as to allow for enzymatic attacks that split larger fibrils into smaller ones.[16] Moreover, as the tensile strength of tendons or ligaments is positively associated with collagen fibril diameter[14,17] and fibril density,[18] a healing tissue with a smaller fibril diameter is unable to fully sustain physiological loading. Consequently, the structural characteristics of the connective tissues, such as collagen fibril diameter and organization are crucial design parameters for biomimetic scaffolds intended for tendon or ligament regeneration.

To date, the effect of scaffold fiber diameter on the response of the resident cell population in tendons or ligaments has not been evaluated. This study focuses on elucidating the mechanism of cell–material interactions by investigating how connective tissue cells, such as tendon fibroblasts respond to scaffolds with different fiber diameters in terms of biosynthesis and differentiation. Here, it is hypothesized that fibroblasts can distinguish differences in scaffold fiber diameters and that their response on micron-

[1]Biomaterials and Interface Tissue Engineering Laboratory, Department of Biomedical Engineering, Columbia University in the City of New York, New York, New York.
[2]Department of Orthopaedic Surgery, Columbia University in the City of New York, New York, New York.

Table 1. Diameter of Collagen Fibrils/Fibers in Healthy and Injured Connective Tissues

Source	*Healthy*	*Injured/healing*	*Authors*
Patellar tendon (human)	72% <60 nm	95% <60 nm	Svensson *et al.*[10]
Supraspinatus tendon (human)	Mean: 57 ± 3 nm	51 ± 3 nm	Wang *et al.*[11]
Patellar tendon (mice)	Mean: 114 ± 38 nm	43 ± 7 nm (2 weeks)	Alaseirlis *et al.*[9]
Patellar tendon (rabbit)	Median: 161 ± 5 nm Range: 30–390 nm	Median: 94.4 ± 19.7 nm Range: 30–360 nm	Majima *et al.*[2]
Tendon (human)	Range: 1–300 μm	—	Silver *et al.*[3]
Achilles tendon (human)	28.5 ± 2.7 μm	18.2 ± 1.0 μm	Jarvinen *et al.*[12]

sized and nano-sized fibers will be analogous to their behavior in healing and healthy tissues in terms of adhesion, matrix synthesis, and gene expression. It is anticipated that the results of this study, the first to use the nanofibers/microfibers as a model system to compare the cell response between healing versus healthy extracellular matrix, will provide new insights into the mechanism of connective tissue healing in addition to identifying biomimetic scaffold design rules for functional connective tissue repair.

Materials and Methods

Scaffold fabrication

The nanofiber and microfiber scaffolds were fabricated by electrospinning. Briefly, 1.00, 1.50, 2.00, or 2.25 g of poly(D,L-lactide-*co*-glycolide) (PLGA, 85:15 DL High IV; Lakeshore Biomaterials) was premixed in 2.75 mL of dimethylformamide, followed by the addition of 0.5 mL of ethanol. This process yielded polymer concentrations of 30%, 46%, 62%, and 70% (g/mL) respectively. The solution viscosity ($n=4$) was measured using a Rheometer (TA Instruments). Specifically, $\sim$2 mL of the sample was subjected to oscillatory strains at room temperature in the range of 1%–100% at 10 radian/s(rps) frequency (using 60 mm parallel plates, 1 mm gap). The zero shear viscosity corresponding to the linear region in the strain range studied at 10 rps frequency was taken as the viscosity of the solution.[19]

In addition, the concentration (i.e., viscosity) or flow-rate of the electrospinning process was modified to fabricate scaffolds with different diameters. More specifically, solutions containing 46% or 70% (weight/volume) PLGA were used to form fibers with two different diameters by electrospinning at 8–10 kV and at a flow rate of 1 mL/h, with the collecting drum rotating at 20 m/s and located at 10.5 cm away from the tip of the needle. To obtain smaller diameter fibers, the 46% PLGA solution was electrospun at a flow-rate of 0.35 mL/h. In this study, scaffolds with diameters averaging 320 ± 100 nm, 680 ± 180 nm, and 1.80 ± 0.16 μm, were fabricated and used to test the response of human rotator cuff tendon fibroblasts (hRCFb).

Scaffold characterization

Scaffolds were imaged by scanning electron microscopy (SEM, 0.8 kV; Hitachi 4700) and fiber diameters were measured using ImageJ (National Institutes of Health). The fiber diameter was determined from the SEM images ($n=3$/group). Briefly, each image was segmented with five vertical lines of equal spacing, and fibers intersecting with the verticals were marked (red circles, in Fig. 1A). The diameter of these fibers were measured by ImageJ, and an average fiber diameter was calculated (averaging $n=50$ fibers per image). In addition, fiber alignment ($n=3$) was measured using circular statistics software[20] customized for evaluating fiber alignment (Fiber3). The circular statistics parameters determined include the mean vector angle, which represents the average fiber alignment in the matrix ($-90° \le \theta \le 90°$, with 0° for horizontal orientation); the mean vector length, which ranges from zero for a randomly distributed sample to unity for an aligned sample ($0 \le r \le 1$); and angular deviation, which characterizes the dispersion of the non-Gaussian angle distribution of the nanofibers (0–40.5°). Specifically, an angular deviation of 0° represents an aligned sample, and 40.5° is indicative of random distribution.

The mechanical properties ($n=6$) of the as-fabricated aligned scaffolds were evaluated under uniaxial tension. Briefly, the scaffolds (5×1 cm) were secured with custom clamps and mounted on a mechanical testing device (Instron; Model 8841) with an average gauge length of 3 cm. The samples were tested to failure at a strain rate of 5 mm/min, with the scaffolds tested along the nanofiber long axis. For each scaffold type, yield strength, ultimate tensile stress and elongation at break were determined, and the elastic modulus was calculated from the linear region of the stress–strain curve.

Cells and cell culture

Human rotator cuff fibroblasts were derived from explant culture of human tendon tissues of patients (50-year-old male and 60-year-old female, institutional review board exempt) who underwent rotator cuff repair surgery. Briefly, the tissue samples were rinsed with phosphate-buffered saline (PBS; Sigma-Aldrich), plated in tissue culture dishes, and maintained in a fully supplemented medium that contained the Dulbecco's modified Eagle's medium plus 10% fetal bovine serum, 1% nonessential amino acids, 1% penicillin/streptomycin, and 1% amphotericin B. The cells from the first migration were subsequently discarded, and the tissue was re-plated in the fully supplemented medium. Only cells obtained from the second and third migrations were used in this study, because this method has been shown to yield a relatively homogenous fibroblast population.[21] All medium and supplements were purchased from Mediatech unless otherwise stated.

To prevent contraction,[22] the scaffolds were secured using custom-made clamps. After ultraviolet sterilization, the scaffolds were preincubated in the fully supplemented medium at 37°C and 5% CO_2 for 16 h. Human rotator cuff fibroblasts (passage 3) were seeded on the scaffolds at a density of 3×10^4 cells/cm^2 and allowed to attach for 15 min before the addition of medium. The cells were cultured on the scaffolds for 4 weeks, with monolayer culture of the human tendon fibroblasts serving as controls. The effects of fiber diameter on cell morphology, attachment, gene expression, proliferation, and matrix production were determined over time.

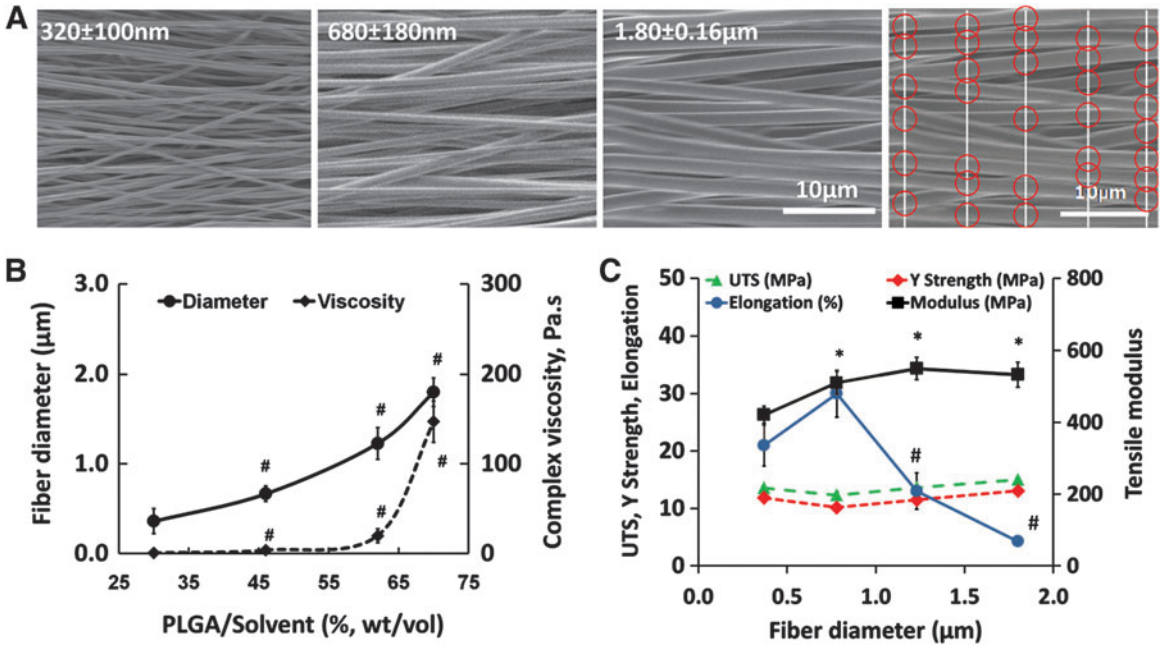

FIG. 1. Effect of diameter on scaffold mechanical properties. **(A)** Nano- and microfiber scaffolds (scanning electron microscopy, 0.8 kV, 2000×). **(B)** Fiber diameter ($n=3$) increased with solution viscosity ($n=4$). **(C)** Effect of fiber diameter on scaffold tensile properties ($n=6$). "#" indicates significant difference within a group at consecutive values of fiber diameter and "*" indicates significant difference as compared to 320 nm at $p<0.05$. Red circles indicate points of measurements. PLGA, poly(D,L-lactide-*co*-glycolide); UTS, ultimate tensile strength. Color images available online at www.liebertpub.com/tea

Cell viability, alignment, and aspect ratio

Cell viability ($n=3$) and attachment morphology were evaluated using live/dead staining (Molecular Probes). The samples were rinsed twice with PBS and stained following the manufacturer's protocol. The samples were imaged under confocal microscopy (Leica TCS SP5) at wavelengths of 488 and 568 nm. Cell alignment ($n=3$) was measured at day 28 following the procedure described above for scaffold alignment. The aspect ratio of cells were determined at day 1, 7, and 28 using confocal images ($n=3$, averaging 50 cells/image). Specifically, the long axis and short axis of an average of 50 cells per image were measured using ImageJ, and the ratio of the axes was reported as the aspect ratio of cells.

Cell proliferation

Cell proliferation ($n=6$) was determined by measuring the total DNA content using the PicoGreen double strand DNA assay (Invitrogen; Product# P11496) following the manufacturer's suggested protocol. At designated time points, each scaffold was rinsed with PBS and homogenized in 0.1% Triton-X solution (Sigma-Aldrich, Cat# T-9284). Fluorescence was measured using a microplate reader (Tecan) at the excitation and emission wavelengths of 485 and 535 nm, respectively. A standard curve was generated to correlate the DNA content with fluorescence intensity, and the number of cells was determined using a conversion factor of 8 pg DNA/cell.[23]

Matrix production

Matrix synthesis ($n=6$) by fibroblasts was evaluated in terms of both glycosaminoglycan (GAG) and collagen production. To quantify the GAG content, a modified 1,9-dimethylmethylene blue (DMMB) dye binding assay[24] with chondroitin-6-sulfate (Sigma) as a standard was used. To account for the anionic nature of the carboxyl groups present in the PLGA scaffolds, the pH of the DMMB dye was adjusted to be 1.5 with the concentrated formic acid (Sigma) so that only the sulfated GAG–DMMB complexes were detectable with the spectrophotometer. The absorbance difference between 540 and 595 nm was used to improve signal detection. Total collagen production was measured using the Sircol Assay (Biocolor) following the manufacturer's suggested protocol. A standard curve was generated to correlate absorbance determined at 555 nm with collagen concentration.

Expression of phenotypic tendon fibroblast markers

Gene expression ($n=4$) was measured using reverse transcriptase–polymerase chain reaction at 3, 7, and 14 days. Total RNA was isolated using the Trizol extraction method (Invitrogen, Cat# 15596-018). The isolated RNA was reverse-transcribed into complementary DNA (cDNA) using the SuperScript First-Strand Synthesis System (Invitrogen), and the cDNA product was then amplified using recombinant Taq DNA polymerase (Invitrogen). Expression of Collagen1α1 (sense, 5′-TGGTCCACTTGCTTGAAGAC-3′, 137 bp; antisense, 5′-ACAGATTTGGGAAGGAGTGG-3′, 137 bp), Collagen3α1 (sense, 5′-CCATTTGGAGAATGTTGTGC-3′, 80 bp; antisense, 5′-CCTTGAGGTCCTTGACCATT-3′, 80 bp), Collagen5α1 (sense, 5′-AGACCACCAAATTCCTCGAC-3′, 104 bp; antisense, 5′-GTCACCCTCAAACACCTCCT-3′, 104 bp), Tenomodulin (sense, 5′-TTTGAGGAGGAGGGAGAAGA-3′, 129 bp; antisense, 5′-TTCCTCACTTGCTTGTCTGG-3′, 129 bp) and matrix metalloproteinase-2 (MMP-2) (sense, 5′-CTGCATCCA GACTTCCTCAG-3′, 74 bp; antisense, 5′-CTGGCAATCCC

TTTGTATGTT-3′, 74 bp) were determined over time. Glyceraldehyde-3-phosphate dehydrogenase (GAPDH) (sense, 5′-ATCATCCCTGCCTCTACTGG-3′, 122 bp; antisense, 5′-GTCAGGTCCACCACTGACAC-3′, 122 bp) served as the house-keeping gene. All genes were amplified for 30 cycles in a thermocycler (Eppendorf Mastercycler gradient; Brinkmann). Semiquantitative analysis of gene expression (ImageJ) was performed, and band intensity was normalized to that of GAPDH.

Statistical analysis

Results are presented in the form of mean ± standard deviation, with n equal to the number of replicates per group. One-way analysis of variance (ANOVA) was performed to determine the effects of solution concentration on the scaffold fiber diameter or viscosity. Two-way ANOVA was used to determine the fiber diameter and temporal effects on cell alignment, cell aspect ratio, proliferation, matrix production, and gene expression. In addition, the effect of the fiber diameter on scaffold tensile mechanical properties (i.e., ultimate tensile strength [UTS], yield strength, elongation, and tensile modulus) was determined using multivariate ANOVA. The Tukey–Kramer *post hoc* test was used for all pairwise comparisons, and significance was attained at $p < 0.05$. Statistical analyses were performed with JMP IN (4.0.4; SAS Institute, Inc.).

Results and Discussion

This study investigates the effects of the substrate fiber diameter on response of the tendon fibroblasts. The polymeric scaffolds were fabricated by electrospinning, a versatile technique routinely utilized to form fibrous scaffolds in the nanometer as well as micrometer ranges[25] by varying material properties and fabrication parameters.[26] Briefly, PLGA (85:15) solutions with designated concentrations were electrospun onto a rotating drum to form aligned nano- and microfiber scaffolds. As expected, the fiber diameter was directly modulated by polymer solution viscosity (Fig. 1B). While scaffold mechanical property values are well within the range of those of major ligaments and tendons,[27] an improved modulus and reduced ductility were observed with an increasing fiber diameter (Fig. 1C). The UTS and yield strength of the scaffolds remained unchanged in the diameter range studied (i.e., 320 nm–1.80 μm); however, a significant increase in the tensile modulus (from 421 ± 23 MPa to 510 ± 32 MPa) was observed with the increasing fiber diameter. Ductility or elongation at break decreased significantly from 30% ± 4.1% to 13% ± 3.2% when the scaffold diameter increased from 680 ± 180 nm to 1.23 ± 0.18 μm, respectively. It is emphasized that scaffolds tested here exhibited physiological levels of mechanical properties[27] as compared with those of tendons and ligaments, and that changes in the fiber diameter could be used to control the scaffold mechanical properties.

Next, to investigate the effect of the fiber diameter on cell response, hRCFb were seeded on scaffolds with an average fiber diameter of either 320 ± 100 nm, 680 ± 180 nm, or 1.80 ± 0.16 μm (Fig. 1A). These diameter groups were selected as the smallest nanofiber tested (320 nm) is similar in diameter to the collagen fibril (360 nm), and is also representative of the scar tissue formed in the repair phase[28,29] of the healing process post injury. The microfiber group (1.80 μm) consists of fibers that are similar in diameter to the collagen fiber (1–300 μm) and within the range of fibers found in healthy tendons or ligaments. Specifically, the cell response was evaluated in terms of cell alignment, aspect ratio, proliferation, biosynthesis (collagen and GAGs), and expression of phenotypic markers, such as collagen I, III, V, and tenomodulin.

It was observed that the attachment of human tendon fibroblasts was guided by both the fiber diameter and organization (Fig. 2A). Fiber and cell orientation analyses[20,27] revealed that the cells perceived the underlying fiber organization and aligned themselves in the direction of the free boundary,[20,30] that is, the long axis of the fibrous matrix. Note that the fiber orientations of the as-fabricated scaffolds

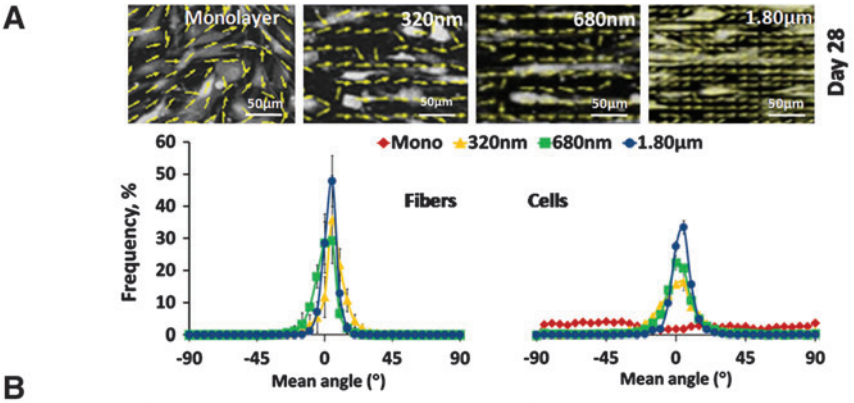

B

	Fibers			Cells		
Fiber Diameter (μm)	Mean Angle (degree)	Angular Deviation (degree)	Mean Vector Length	Mean Angle (degree)	Angular Deviation (degree)	Mean Vector Length
Monolayer	–	–	–	78.91±8.71	35.25±2.75	0.24±0.12
0.32±0.10	2.57±1.04	15.69±0.63	0.83±0.05	1.75±0.27#	20.07±1.64#	0.75±0.04#
0.68±0.18 *	2.62±0.72	12.94±3.58	0.89±0.05	1.00±0.10 #*	16.02±0.43 #*	0.84±0.01 #*
1.80±0.16 *^	2.25±1.00	17.15±1.76	0.82±0.04	1.73±0.25 #^	8.21±1.13 #*^	0.96±0.01 #*^

FIG. 2. Fiber diameter guided fibroblast morphology and attachment. **(A)** Top panel: vector maps of cells at day 28; bottom panel: mean angle distribution of fibers and cells at day 28. **(B)** Values of orientation parameters at day 28. #,* and ^ indicate significant difference with respect to monolayer, 320 and 680 nm, respectively, at $p < 0.05$ ($n = 3$). Mean angle: $-90° \le \theta \le 90°$, 0° = horizontal orientation; angular deviation: 0° = aligned, 40.5° = random; mean vector length: 0 = random, 1 = aligned. Color images available online at www.liebertpub.com/tea

were predesigned to be independent of diameter, with no significant difference in terms of mean angle, angular standard deviation, and mean vector length between the scaffolds with different fiber diameters (Fig. 2B). Therefore, any changes in the cell response observed here could be attributed solely to differences in the fiber diameter. It is interesting to note that, in spite of being seeded on an aligned matrix, the tendon fibroblasts exhibited significant ($p<0.05$) differences in alignment as a function of the scaffold fiber diameter (Fig. 2B). Specifically, at day 28, the angular deviation decreased (from 20.07 to 8.21) and the mean vector length increased (from 0.75 to 0.96) with the increasing fiber diameter (from 320 nm to 1.80 μm), collectively demonstrating that the cells are significantly ($p<0.05$) more aligned on scaffolds with larger fibers (1.80 μm).

In the native tendon tissue, fibroblasts are known to exhibit a spindle-shaped, elongated morphology within the confines of bundles of collagen fibrils.[31] In this study, as seen in the cell aspect ratio results (long axis/short axis, Fig. 3B), over time, cells elongated to a greater extent on scaffolds with a large fiber diameter ($p<0.05$). In previous studies, human dermal fibroblasts cultured on aligned poly(methylmethacrylate) fibers (0.16–8.64 μm)[32] and bone marrow-derived stem cells (BMSCs) cultured on aligned polyurethane meshes (0.28–2.3 μm)[33] exhibited a similar response in terms of the cell aspect ratio. Here, while no difference was found among the groups at day 1, the aspect ratios of cells by day 7 were 5.81 ± 0.40, 7.11 ± 0.98, and 9.22 ± 0.56 on scaffolds with diameters of 320 nm, 680 nm, and 1.80 μm, respectively. Similar variations between the groups were also observed at day 28 (Fig. 3B). The relatively lower aspect ratio of cells on smaller fibers is likely because the cells could more readily spread on nanofiber scaffolds as compared to microfiber

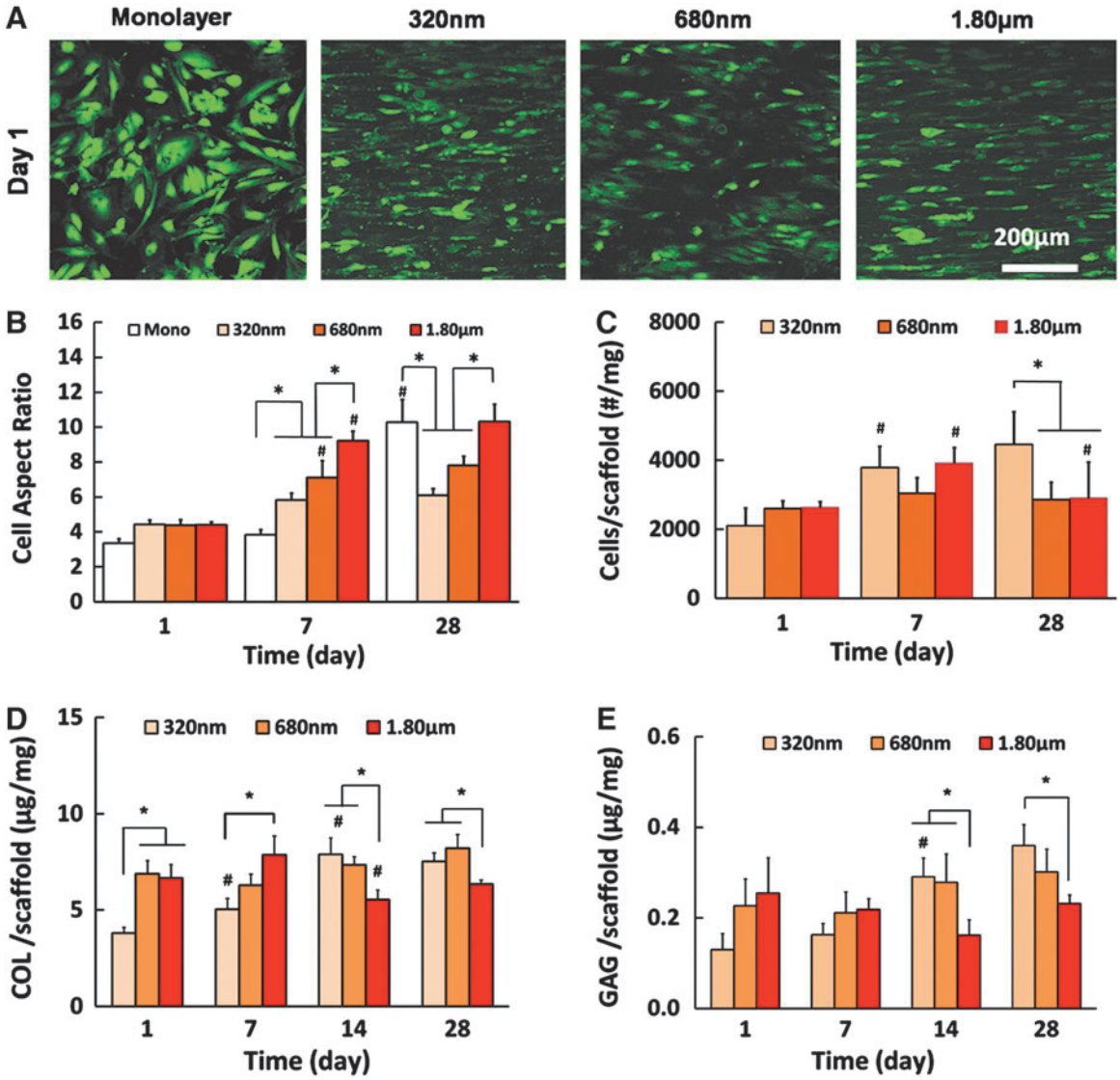

FIG. 3. Effect of scaffold fiber diameter on cell biosynthesis. **(A)** Cell viability (live/dead, $n=3$). **(B)** Aspect ratio of cells over time ($n=3$). **(C)** Cell proliferation ($n=6$). **(D)** Collagen production ($n=6$), and **(E)** Glycosaminoglycan (GAG) production ($n=6$). * and # indicate significant difference between groups at a given time point and within a group at consecutive time points, respectively, at $p<0.05$. Color images available online at www.liebertpub.com/tea

scaffolds due to smaller depth of grooves with a higher fiber density.[34]

It was observed here that tendon fibroblasts remained viable on all substrates tested (Fig. 3A), although a significantly greater cell number was found on the scaffolds with the small diameter fibers (320 nm) as compared with 680 nm and 1.80 μm groups (Fig. 3C, $p < 0.05$). Previously, proliferation of BMSCs[33] and NIH 3T3 fibroblasts[35] have been reported to be unaffected by the fiber diameter when these cells were cultured on the aligned polyurethane fibers (0.28–2.3 μm) and PLGA 75:25 fibers (0.14–3.6 μm), respectively. This may be due to differences in cell types as well as the chemistry of scaffold material. Interestingly, fibroblasts synthesized more collagen (Fig. 3D, $p < 0.05$) and proteoglycans (Fig. 3E, $p < 0.05$) on scaffolds with a smaller fiber diameter. When normalized by the cell number, while collagen production per cell was comparable between the groups, a significantly higher proteoglycan deposition per cell was found on the nanofiber scaffolds. This difference in biosynthesis is significant because collagen and proteoglycan are the major components of connective tissues, such as tendons and ligaments. For example, the human supraspinatus tendon has been reported to contain 9.63% collagen[36] and 1.23% sulfated GAGs[37] based on dry weight. It was observed here that by day 28, tendon fibroblasts also produced a matrix richer in collagen (0.75 ± 0.04 wt% on 320 nm scaffolds vs. 0.64 ± 0.02 wt% on 1.80 μm scaffolds) as compared to GAG (0.036 ± 0.005 wt% on 320 nm scaffolds vs. 0.023 ± 0.002 wt% on 1.80 μm scaffolds). It is possible that, to the tendon fibroblasts, the scaffolds with a smaller fiber diameter resemble a matrix in the state of injury and the cells, therefore, initiated a healing response by producing more matrix components, such as proteoglycans. In contrast, the scaffolds with larger fibers likely approximate the fiber diameter of a healthy tendon matrix, and the cells would, therefore, minimize excess matrix deposition. It is noted that the progressive increase in the scaffold diameter tested here may also be representative of matrix changes during the healing process. Williams *et al.*[38] reported a moderate recovery of the fibrillar structure, which took place during 14 months after an acute traumatic injury in rats, although the collagen fibril diameter remained abnormally low compared to the native tissue. In this study, a cell response to the intermediate diameter group (680 nm) was a mixture of those observed on the smallest and largest fibers, suggesting a potential progression in cells response if the fibril assembly into fibers can proceed normally.

Cell differentiation was assessed by examining the effects of the fiber diameter on temporal expressions of phenotypic markers, including collagen I, III, V, and tenomodulin (Fig. 4). In general, expressions of these markers were at the basal level for monolayer control, and nanofiber scaffolds. Specifically, at day 3, collagen I and V expressions were significantly lower on scaffolds with the largest fiber diameter (1.80 μm), while tenomodulin expression was comparable on all substrates. By day 7, only collagen V expression was lower on the largest fibers. By day 14, however, the fibroblasts on microfiber scaffolds (1.80 μm) expressed the highest levels of collagen I, III, V, and tenomodulin. It is seen from the matrix production results that collagen production decreased significantly by day 14 on the largest diameter scaffolds (Fig. 3D). Therefore, it is possible that cells are upregulating these markers in response to the observed decrease in collagen synthesis. To further investigate the response of tendon cells on scaffolds with different diameters, MMP-2 expression was also evaluated to determine if cell-mediated collagen degradation was evident (Fig. 4). Matrix remodeling plays a critical role and the balance between the activities of MMPs and tissue inhibitors of MMPs regulates tendon remodeling in both healthy and injured tissues.[39,40] However, no fiber diameter-related changes in MMP-2 expression were observed in this study within the time frame examined.

The collagen III to collagen I expression ratio was also calculated over a period of 2 weeks. This ratio is one of the major indicators of the dynamics of tissue response to injury, averaging 0.1 for a healthy tissue and becomes elevated at the time of injury. The ratio is known to be restored to baseline with time as the injured tendons remodel and heal.[41,42] In this study, a significant decrease in the ratio of collagen III to collagen I expressions (from 0.92 to 0.63, $p < 0.05$) was measured on the largest diameter scaffolds (1.80 μm) at day 7 as compared with day 3 (Table 2). This again may reflect a state of the healthier tendon matrix and may be attributed to the biomimicry of the scaffolds with large diameter fibers. It should be noted that although the collagen fibril diameter in tendons ranges between 20 and several hundreds of nanometers (Table 1), the diameter of bundles of these fibrils, that is, collagen fibers, in which the cells are elongated and closely packed, can be as high as 1–300 μm.[3] Therefore, it is likely that the interaction between microfiber (1.80 μm) scaffolds and fibroblasts of this study more closely resembles what is occurring in native environment and that microfiber scaffolds better approximate the collagen fibers of the native tendon.

Moreover, the higher level of collagen V expression on the larger fibers could be taken as an indication of initiation of the collagen fibril assembly within the 1.80 μm fiber scaffolds. Collagen V was reported to be the earliest deposited molecule and to serve as a nucleating agent for the short primary fibrils in fibril formation.[43,44] The effect of collagen V in the fibril assembly was investigated by Wenstrup *et al.*[43] using a Col5a1-deficient mice model, and it was found that collagen V is the most effective matrix component in initiating fibrillogenesis. It is suggested that the mechanism of action of collagen V starts with its deposition at the surface of connective tissue cells, generating short primary fibrils and continues with the enlargement of these structures upon side-by-side and end-to-end fusion to form collagen fibrils. Based on results of this study, it is possible that the cells first oriented themselves in the direction of microfibers, exhibiting their characteristic elongated morphology, and then upregulated collagen V expression to initiate fibril formation and matrix assembly. Similarly, tenomodulin is a recently identified type II transmembrane protein,[45] expressed predominantly by the cells of tendons and ligaments,[46] and is known to play a role in regulating the formation of collagen fibrils with uniform sizes and smooth surfaces.[47] The upregulation of tenomodulin expression on the 1.80 μm group by day 14 suggests that here, the largest fiber diameter scaffolds favored the formation of a more tendon-like matrix. While an altered cell response precipitated by injury is anticipated at the wound site, the results of this study demonstrate that the persistence of a small nanofiber-sized matrix at the healing

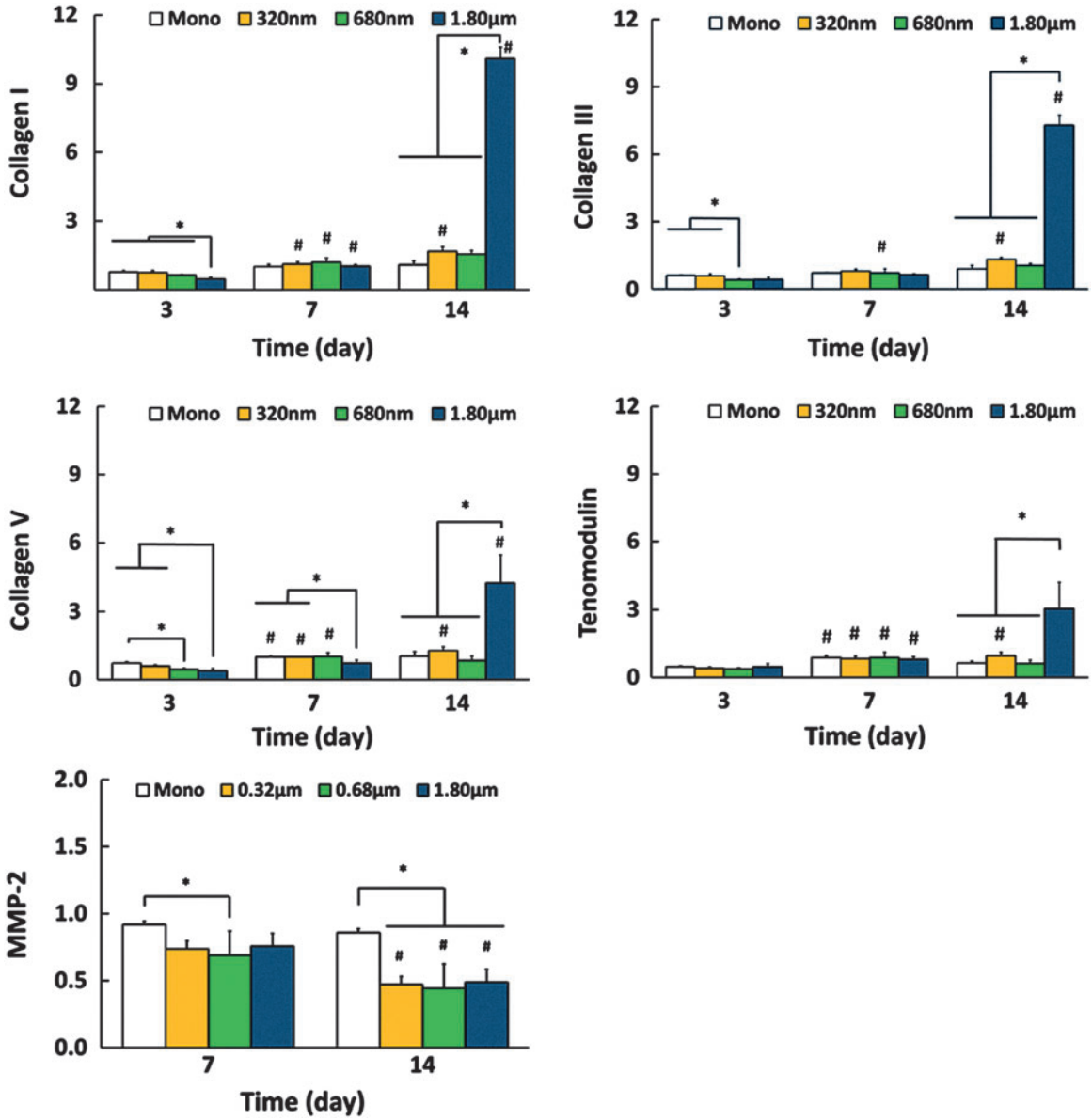

FIG. 4. Expression of Col I, Col III, Col V, tenomodulin, and matrix metalloproteinase-2 (MMP-2) by human rotator cuff tendon fibroblasts cells. * and # indicate significant difference between groups at a given time point and within a group at consecutive time points, respectively, at $p < 0.05$ ($n = 4$). Color images available online at www.liebertpub.com/tea

site promotes scar tissue formation and is likely not conducive to the reformation of a functional tendon matrix.

To the best of our knowledge, there is no reported study on the effect of fiber diameter on either tendon or ligament fibroblast response. However, the expression of collagen I, III, and tenomodulin on fibers with comparable diameters, but using different cell types have been evaluated. For example, human dermal fibroblasts[48] cultured on unaligned scaffolds (poly[lactic acid-*co*-glycolic acid], 50:50) exhibited by day 7 a similar response as tendon fibroblasts of this study with both remaining unaffected by the fiber diameter in terms of expressing collagen I and collagen III. At day 14, however, dermal fibroblasts downregulated the expression of collagen III on the scaffolds with fiber diameters between 2.5 and 3.0 μm, while tendon fibroblasts upregulated both collagen I and collagen III on scaffolds with a mean diameter of 1.80 μm. These differences are likely due to the cell type and the use of aligned nanofibers in this study. Recently, Bashur *et al.* reported that at day 7, rat BMSCs expressed a lower level of Col1α1 on aligned polyurethane scaffolds with diameters of 0.82 or 2.3 μm as compared to 0.28 μm.[33] In contrast, collagen I was upregulated in this study for tendon

Table 2. Collagen III to Collagen I Expression Ratio

Time (day)	*Monolayer*	*320 nm*	*680 nm*	*1.80 μm*
3	0.83 ± 0.04	0.87 ± 0.04	0.68 ± 0.10	0.92 ± 0.22
7	0.76 ± 0.07	0.71 ± 0.06	0.54 ± 0.16	0.63 ± 0.09*
14	0.78 ± 0.01	0.86 ± 0.05	0.66 ± 0.02	0.66 ± 0.08

*Indicates significance with respect to previous time point, $p < 0.05$.

fibroblasts cultured on the largest fibers (1.80 μm) by day 14. In terms of tenomodulin, a similar upregulation was found at day 7 for rat BMSCs cultured on polyurethane fibers with diameters of 0.28, 0.82, and 2.3 μm,[33] although tendon fibroblasts expressed the highest level of tenomodulin on the largest fibers (1.80 μm) by day 14. These differences are likely due to the cell type (rat BMSCs vs. human tendon fibroblasts) and cell seeding density ($5\times10^3/cm^2$ vs. $30\times10^3/cm^2$ in this study). It is emphasized that the tendon matrix repair is reported to begin a few days after the injury and to persist up to 6 weeks,[29] with both tendon fibroblasts and progenitor or stem cells actively participating in this process. Future studies will compare the response of human MSCs with those of tendon fibroblasts as a function of fiber diameter.

In this study, while the tensile modulus of the scaffolds increased significantly with an increasing fiber diameter (i.e., 421 ± 23 MPa for 320 nm to 510 ± 32 MPa for 1.8 μm), these differences are not expected to contribute significantly to the observed effects on cell response, mainly because the PLGA fiber matrix tested here is much stronger than the cell or its local matrix. Published studies demonstrating the effect of substrate stiffness on cell response have confined to matrices with elastic moduli in the low kPa range, which is reasonable given that fibroblast stiffness is reported to average 1–8 kPa depending on substrate rigidity.[49] Moreover, Tan and Lim[50] reported that while the elastic modulus of a single electrospun poly(L-lactic acid) (PLLA) nanofiber is lower compared with the PLLA bulk, it is still within the same order of magnitude (i.e., 1 ± 0.2 GPa for a single 340 nm fiber vs. 1–10 GPa for PLLA bulk). Therefore, for this study, it is not expected that the cells would be able to significantly deform the PLGA substrate, even at the single fiber level. Consequently, the observed differences in cell responses are more likely to be a result of changes in the fiber diameter.

Collectively, the results of this study reveal that, within the range studied, the fiber diameter modulated tendon fibroblast attachment, growth, biosynthesis, and differentiation. In general, while the nanofibers (320 nm) enhanced matrix synthesis, the microfibers (1.8 μm) promoted cell alignment and phenotypic expression that will likely lead to the deposition of a more tendon-like matrix. Therefore, the nanofiber-scale scaffolds may resemble the matrix in a state of injury, stimulating the cells for matrix deposition as a part of the repair process, while microfibers represent the assembled, healthy matrix with micron-sized collagen bundles, thereby inducing cells to differentiate. In addition, given the dynamic remodeling state of connective tissues, it is possible that a scaffold exhibiting a bimodal diameter distribution could serve as a more appropriate environment, where both matrix production and cell differentiation can be accomplished. Such a scaffold design could lead to repopulation of cells and production of relevant matrix components at the injury site due to the presence of nanofibers, while at the same time modulating the expression of related phenotypic markers for improved tendon healing as a response to the presence of micron-sized fibers. It is emphasized that as fiber diameter effects on ligament or tendon fibroblasts have not been extensively studied, this study was designed as a relatively simple system and investigation of the effects of bimodal fiber distribution on the cell response is planned in future studies. In this study, the cells used were not presorted to synchronize cell cycle/state. Given that the cell population present at the healing site is also nonhomogenous, and likely in different stages of cell cycle, it is anticipated that the response observed here is still representative. As such, an in-depth investigation of the effects of cell state on the observed responses is planned in future studies. Moreover, the clinical significance of these observed effects of the scaffold fiber diameter will be validated *in vivo* using relevant soft tissue injury models in future studies.

Conclusions

Overall, this study evaluated the response of human tendon fibroblasts on aligned polymeric scaffolds with different fiber diameters, averaging 320 nm, 680 nm, and 1.80 μm. It was evident that fiber diameter regulates scaffold mechanical properties as well as cell response *in vitro*. In addition, the higher cell growth, collagen, and GAG production observed on the nanofibers versus the upregulation of phenotypic markers of tendon fibroblasts, such as collagen I, III, V, and tenomodulin on microfibers clearly demonstrate the effect of structural properties of scaffolds on cell behavior, and delineate the importance of fiber diameter as a design parameter in the fabrication of biomimetic scaffolds. These findings also provide new insights into cell–material interactions that are critical for understanding the mechanism of connective tissue repair, in particular, the role of matrix parameters, such as the fiber diameter in guiding cell response and eventual healing. In addition to serving as a model system, the design attributes of the scaffolds tested in this study are critical for guided and functional connective tissue regeneration. The results of this study highlight the importance of strategic biomimicry as a scaffold design principle for eliciting desired cellular responses, which depending on clinical need, could be either enhanced matrix deposition and or upregulation of phenotypic markers.

Acknowledgments

The authors gratefully acknowledge funding support from the National Institutes of Health/National Institute of Arthritis and Musculoskeletal and Skin Diseases (AR052402, AR056459, and AR055280) and New York State Stem Cell Initiative (NYSTEM).

Disclosure Statement

No competing financial interests exist.

References

1. Yang, L., van der Werf, K.O., Fitie, C.F., Bennink, M.L., Dijkstra, P.J., and Feijen, J. Mechanical properties of native and cross-linked type I collagen fibrils. Biophys J **94,** 2204, 2008.
2. Majima, T., Yasuda, K., Tsuchida, T., Tanaka, K., Miyakawa, K., Minami, A., and Hayashi, K. Stress shielding of patellar tendon: effect on small-diameter collagen fibrils in a rabbit model. J Orthop Sci **8,** 836, 2003.
3. Silver, F.H., Kato, Y.P., Ohno, M., and Wasserman, A.J. Analysis of mammalian connective tissue: relationship between hierarchical structures and mechanical properties. J Long Term Eff Med Implants **2,** 165, 1992.
4. Kannus, P. Structure of the tendon connective tissue. Scand J Med Sci Sports **10,** 312, 2000.

5. Gulotta, L.V., and Rodeo, S.A. Growth factors for rotator cuff repair. Clin Sports Med **28,** 13, 2009.
6. Griffin, L.Y., Agel, J., Albohm, M.J., Arendt, E.A., Dick, R.W., Garrett, W.E., Garrick, J.G., Hewett, T.E., Huston, L., Ireland, M.L., Johnson, R.J., Kibler, W.B., Lephart, S., Lewis, J.L., Lindenfeld, T.N., Mandelbaum, B.R., Marchak, P., Teitz, C.C., and Wojtys, E.M. Noncontact anterior cruciate ligament injuries: risk factors and prevention strategies. J Am Acad Orthop Surg **8,** 141, 2000.
7. Frank, C., McDonald, D., and Shrive, N. Collagen fibril diameters in the rabbit medial collateral ligament scar: a longer term assessment. Connect Tissue Res **36,** 261, 1997.
8. Galatz, L.M., Ball, C.M., Teefey, S.A., Middleton, W.D., and Yamaguchi, K. The outcome and repair integrity of completely arthroscopically repaired large and massive rotator cuff tears. J Bone Joint Surg Am **86-A,** 219, 2004.
9. Alaseirlis, D.A., Li, Y., Cilli, F., Fu, F.H., and Wang, J.H. Decreasing inflammatory response of injured patellar tendons results in increased collagen fibril diameters. Connect Tissue Res **46,** 12, 2005.
10. Svensson, M., Movin, T., Rostgard-Christensen, L., Blomen, E., Hultenby, K., and Kartus, J. Ultrastructural collagen fibril alterations in the patellar tendon 6 years after harvesting its central third. Am J Sports Med **35,** 301, 2007.
11. Wang, V.M., Wang, F.C., McNickle, A.G., Friel, N.A., Yanke, A.B., Chubinskaya, S., Romeo, A.A., Verma, N.N., and Cole, B.J. Medial versus lateral supraspinatus tendon properties: implications for double-row rotator cuff repair. Am J Sports Med **38,** 2456, 2010.
12. Jarvinen, T.A., Jarvinen, T.L., Kannus, P., Jozsa, L., and Jarvinen, M. Collagen fibres of the spontaneously ruptured human tendons display decreased thickness and crimp angle. J Orthop Res **22,** 1303, 2004.
13. Strocchi, R., De Pasquale, V., Facchini, A., Raspanti, M., Zaffagnini, S., and Marcacci, M. Age-related changes in human anterior cruciate ligament (ACL) collagen fibrils. Ital J Anat Embryol **101,** 213, 1996.
14. Frank, C.B., Hart, D.A., and Shrive, N.G. Molecular biology and biomechanics of normal and healing ligaments—a review. Osteoarthritis Cartilage **7,** 130, 1999.
15. Waggett, A.D., Ralphs, J.R., Kwan, A.P., Woodnutt, D., and Benjamin, M. Characterization of collagens and proteoglycans at the insertion of the human Achilles tendon. Matrix Biol **16,** 457, 1998.
16. Moeller, H.D., Bosch, U., and Decker, B. Collagen fibril diameter distribution in patellar tendon autografts after posterior cruciate ligament reconstruction in sheep: changes over time. J Anat **187 (Pt 1),** 161, 1995.
17. Christiansen, D.L., Huang, E.K., and Silver, F.H. Assembly of type I collagen: fusion of fibril subunits and the influence of fibril diameter on mechanical properties. Matrix Biol **19,** 409, 2000.
18. Battaglia, T.C., Clark, R.T., Chhabra, A., Gaschen, V., Hunziker, E.B., and Mikic, B. Ultrastructural determinants of murine achilles tendon strength during healing. Connect Tissue Res **44,** 218, 2003.
19. Degirmenbasi, N., Kalyon, D.M., and Birinci, E. Biocomposites of nanohydroxyapatite with collagen and poly(vinyl alcohol). Colloids Surf B Biointerfaces **48,** 42, 2006.
20. Costa, K.D., Lee, E.J., and Holmes, J.W. Creating alignment and anisotropy in engineered heart tissue: role of boundary conditions in a model three-dimensional culture system. Tissue Eng **9,** 567, 2003.
21. Lu, H.H., Cooper, J.A., Jr., Manuel, S., Freeman, J.W., Attawia, M.A., Ko, F.K., and Laurencin, C.T. Anterior cruciate ligament regeneration using braided biodegradable scaffolds: *in vitro* optimization studies. Biomaterials **26,** 4805, 2005.
22. Spalazzi, J.P., Vyner, M.C., Jacobs, M.T., Moffat, K.L., and Lu, H.H. Mechanoactive scaffold induces tendon remodeling and expression of fibrocartilage markers. Clin Orthopaed Relat Res **466,** 1938, 2008.
23. Jiang, J., Nicoll, S.B., and Lu, H.H. Co-culture of osteoblasts and chondrocytes modulates cellular differentiation *in vitro*. Biochem Biophys Res Commun **338,** 762, 2005.
24. Farndale, R.W., Sayers, C.A., and Barrett, A.J. A direct spectrophotometric microassay for sulfated glycosaminoglycans in cartilage cultures. Connect Tissue Res **9,** 247, 1982.
25. Erisken, C., Kalyon, D.M., Wang, H.J., Ornek-Ballanco, C., and Xu, J.H. Osteochondral tissue formation through adipose-derived stromal cell differentiation on biomimetic polycaprolactone nanofibrous scaffolds with graded insulin and beta-glycerophosphate concentrations. Tissue Eng Part A **17,** 1239, 2011.
26. Demir, M.M., Yilgor, I., and Erman, B. Electrospinning of polyurethane fibers. Polymer **43,** 3303, 2002.
27. Moffat, K.L., Kwei, A.S., Spalazzi, J.P., Doty, S.B., Levine, W.N., and Lu, H.H. Novel nanofiber-based scaffold for rotator cuff repair and augmentation. Tissue Eng Part A **15,** 115, 2009.
28. Killian, M.L., Cavinatto, L., Galatz, L.M., and Thomopoulos, S. The role of mechanobiology in tendon healing. J Shoulder Elbow Surg **21,** 228, 2012.
29. Wang, J.H. Mechanobiology of tendon. J Biomech **39,** 1563, 2006.
30. Jones, B.F., Wall, M.E., Carroll, R.L., Washburn, S., and Banes, A.J. Ligament cells stretch-adapted on a microgrooved substrate increase intercellular communication in response to a mechanical stimulus. J Biomech **38,** 1653, 2005.
31. Dahlgren, L.A. Pathobiology of tendon and ligament injuries. Clin Tech Equine Pract **6,** 168, 2007.
32. Liu, Y., Ji, Y., Ghosh, K., Clark, R.A., Huang, L., and Rafailovich, M.H. Effects of fiber orientation and diameter on the behavior of human dermal fibroblasts on electrospun PMMA scaffolds. J Biomed Mater Res A **90,** 1092, 2009.
33. Bashur, C.A., Shaffer, R.D., Dahlgren, L.A., Guelcher, S.A., and Goldstein, A.S. Effect of fiber diameter and alignment of electrospun polyurethane meshes on mesenchymal progenitor cells. Tissue Eng Part A **15,** 2435, 2009.
34. Clark, P., Connolly, P., Curtis, A.S., Dow, J.A., and Wilkinson, C.D. Topographical control of cell behaviour: II. Multiple grooved substrata. Development **108,** 635, 1990.
35. Bashur, C.A., Dahlgren, L.A., and Goldstein, A.S. Effect of fiber diameter and orientation on fibroblast morphology and proliferation on electrospun poly(D,L-lactic-co-glycolic acid) meshes. Biomaterials **27,** 5681, 2006.
36. Riley, G.P., Harrall, R.L., Constant, C.R., Chard, M.D., Cawston, T.E., and Hazelman, B.L. Tendon degeneration and chronic shoulder pain: changes in the collagen composition of the human rotator cuff tendons in rotator cuff tendinitis. Ann Rheum Dis **53,** 359, 1994.
37. Riley, G.P., Harrall, R.L., Constant, C.R., Chard, M.D., Cawston, T.E., and Hazelman, B.L. Glycosaminoglycans of human rotator cuff tendons: changes with age and in chronic rotator cuff tendinitis. Ann Rheum Dis **53,** 367, 1994.
38. Williams, I.F., Craig, A.S., Parry, A.D., Goodship, A.E., Shah, J., and Silver, I.A. Development of collagen fibril organiza-

tion and collagen crimp patterns during tendon healing. Int J Biol Macromol **7,** 275, 1985.
39. Dalton, S., Cawston, T.E., Riley, G.P., Bayley, I.J., and Hazleman, B.L. Human shoulder tendon biopsy samples in organ culture produce procollagenase and tissue inhibitor of metalloproteinases. Ann Rheum Dis **54,** 571, 1995.
40. Foos, M.J., Hickox, J.R., Mansour, P.G., Slauterbeck, J.R., and Hardy, D.M. Expression of matrix metalloprotease and tissue inhibitor of metalloprotease genes in human anterior cruciate ligament. J Orthop Res **19,** 642, 2001.
41. Vunjak-Novakovic, G., Altman, G., Horan, R., and Kaplan, D.L. Tissue engineering of ligaments. Annu Rev Biomed Eng **6,** 131, 2004.
42. Wei, A.S., Callaci, J.J., Juknelis, D., Marra, G., Tonino, P., Freedman, K.B., and Wezeman, F.H. The effect of corticosteroid on collagen expression in injured rotator cuff tendon. J Bone Joint Surg Am **88,** 1331, 2006.
43. Wenstrup, R.J., Florer, J.B., Brunskill, E.W., Bell, S.M., Chervoneva, I., and Birk, D.E. Type V collagen controls the initiation of collagen fibril assembly. J Biol Chem **279,** 53331, 2004.
44. Wenstrup, R.J., Smith, S.M., Florer, J.B., Zhang, G., Beason, D.P., Seegmiller, R.E., Soslowsky, L.J., and Birk, D.E. Regulation of collagen fibril nucleation and initial fibril assembly involves coordinate interactions with collagens V and XI in developing tendon. J Biol Chem **286,** 20455, 2011.
45. Shukunami, C., Oshima, Y., and Hiraki, Y. Molecular cloning of tenomodulin, a novel chondromodulin-I related gene. Biochem Biophys Res Commun **280,** 1323, 2001.
46. Brandau, O., Meindl, A., Fassler, R., and Aszodi, A. A novel gene, tendin, is strongly expressed in tendons and ligaments and shows high homology with chondromodulin-I. Dev Dyn **221,** 72, 2001.
47. Docheva, D., Hunziker, E.B., Fassler, R., and Brandau, O. Tenomodulin is necessary for tenocyte proliferation and tendon maturation. Mol Cell Biol **25,** 699, 2005.
48. Kumbar, S.G., Nukavarapu, S.P., James, R., Nair, L.S., and Laurencin, C.T. Electrospun poly(lactic acid-co-glycolic acid) scaffolds for skin tissue engineering. Biomaterials **29,** 4100, 2008.
49. Solon, J., Levental, I., Sengupta, K., Georges, P.C., and Janmey, P.A. Fibroblast adaptation and stiffness matching to soft elastic substrates. Biophys J **93,** 4453, 2007.
50. Tan, E.P.S., and Lim, C.T. Physical properties of a single polymeric nanofiber. Appl Phys Lett **84,** 1603, 2004.

Address correspondence to:
Helen H. Lu, PhD
Biomaterials and Interface Tissue Engineering Laboratory
Department of Biomedical Engineering
Columbia University in the City of New York
351 Engineering Terrace
1210 Amsterdam Avenue
Mail Code: 8904
New York, NY 10027

E-mail: hhlu@columbia.edu

Received: February 5, 2012
Accepted: September 19, 2012
Online Publication Date: November 13, 2012